Two-dimensional model of thermal smoothing of laser imprint in a double-pulse plasma

A. B. Iskakov and V. F. Tishkin
Institute of Mathematical Modeling, Miusskaya Square 4a, 125047 Moscow, Russia

I. G. Lebo
Lebedev Physics Institute, Leninskiy prospekt 53, 117924 Moscow, Russia

J. Limpouch*
Faculty of Nuclear Sciences and Physical Engineering, Czech Technical University in Prague, Břehová 7, 115 19 Praha 1, Czech Republic

K. Mašek and K. Rohlena
Institute of Physics of the Academy of Sciences of the Czech Republic, Na Slovance 2, 180 40 Praha 8-Libeň, Czech Republic
(Received 17 November 1998; revised manuscript received 18 June 1999)

The laser prepulse effect on the thermal smoothing of nonuniformities of target illumination is studied by means of a two-dimensional Lagrangian hydrodynamics simulation, based on the parameters of a real experiment. A substantial smoothing effect is demonstrated for the case of an optimum delay between the prepulse and the main heating laser pulse. The enhancement of the thermal smoothing effect by the laser prepulse is caused by the formation of a long hot layer between the region of laser absorption and the ablation surface. A comparison with experimental results is presented.

PACS number(s): 52.58.Ns, 52.40.Nk, 52.65.−y

I. INTRODUCTION

A very smooth ablation pressure profile (typically up to a few percent) is required in inertial fusion studies to suppress the onset and a subsequent growth of a Rayleigh-Taylor instability, which might disrupt the target compression. The ablation pressure inhomogeneity arises in direct drive experiments of laser inertial fusion due to an inhomogeneous illumination of the target by the heating laser beams. As it is generally very difficult to meet the required homogeneity in the ablation pressure by an improvement of the illumination profile, other smoothing mechanisms have been proposed which are based on a modification of the laser-target interaction.

A powerful intrinsic smoothing mechanism is hidden in the plasma itself, due to the presence of a heat conduction zone between the region of laser absorption and the ablation surface [1–5]. The laser beam energy, which is deposited in the underdense plasma and in the vicinity of the critical surface, is then transported to the target by heat conduction. The thermal transport takes place not only in the longitudinal direction, but also in the transverse direction. Any inhomogeneity in the distribution of the absorbed energy has, thus, a tendency to be washed out when the heat is conducted across the conduction zone. The distance between the absorption region and the ablation surface is controlled by stretching the space between the target and the absorption region. This can be done either by covering the target with a coating of a low density plastic foam [5–8] or by using a laser or x-ray prepulse, which produces an underdense plasma layer prior to the arrival of the main laser pulse. A prepulse technique has also been successfully applied in x-ray laser work. There the purpose of the prepulse is somewhat different; it is used to preform a long smooth plasma profile with a minimum refraction of the amplified x-ray laser beam [9,10]. Consequently, the prepulse or a sequence of prepulses [11] in this case is much weaker than the main pulse, preceding the main pulse typically by 10 ns.

The smoothing by a laser prepulse has been demonstrated by using an iodine laser driver with potassium dideuterium phosphate (DKDP) conversion crystals transforming the laser beam to second and third harmonics [12]. A beam of the second harmonics (red) emission serves as a prepulse followed by the main pulse, formed by the third harmonics beam (blue). In order to simulate the inhomogeneity, the main pulse (blue beam) was split into two foci, which were placed inside a larger red prepulse spot, following a scheme originally proposed by Garanin [12]; see Fig. 1.

The main pulse with an energy of 7 J was split equally into two focal spots, with 80% of the energy confined inside the 20-μm radius. The distance between the spot centers was 80 μm. The circular focus of the prepulse (red beam) contained 80% of its energy (12 J) inside a radius of 100 μm. Both laser pulses were incident normally onto a 7-μm Al foil. The temporal shape of both the laser pulses was close to a Gaussian form with a pulse duration of 0.5-ns full width at half maximum. Three delays (0, 0.5, and 1 ns) of the main pulse, with respect to the prepulse, were used.

In the following, results of two-dimensional (2D) hydrodynamics simulations of ablation pressure smoothing by a laser prepulse are presented and compared with the experimental results [12]. A cylindrical version of Lagrangian code ATLANT [13] is employed for the simulation with the parameters of the model derived from an experiment [12] of

*Author to whom correspondence should be addressed. Electronic address: limpouch@lilit.fjfi.cvut.cz

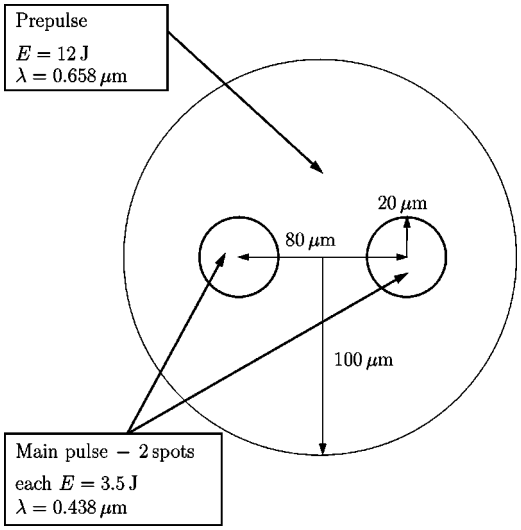

FIG. 1. Target illumination scheme in the experiment when the second (prepulse) and third harmonics (main pulse) of an iodine laser are focused on an Al foil.

double-pulse illumination of Al target foil by an iodine laser. Since the geometry of the code is restricted to a cylindrical symmetry, this study is limited to a model of the smoothing of the ablation pressure induced by a single blue laser spot on the background of a much broader red prepulse. A reduction in the hydrodynamics instability growth in the spherical geometry induced by a laser prepulse with a longer wavelength than the wavelength of the main pulse was reported previously [14]. To our knowledge, no systematic 2D hydrodynamic modeling of a symmetrizing influence of a prepulse of a different color was reported previously.

II. NUMERICAL MODEL

The interaction of two laser pulses with a planar Al solid foil is simulated in a cylindrical geometry. While a Gaussian radial profile is assumed for the main laser pulse (a single blue spot), both uniform and Gaussian radial profiles are used for the laser prepulse (a red beam). The results for a uniform prepulse radial distribution are mainly presented here in order to simplify the comparison of the results for different main pulse delays by avoiding nonuniformities induced by the prepulse. The growth of inhomogeneities in target acceleration is also presented for Gaussian radial profile of the prepulse, and the optimum delay is used to demonstrate the impact of the prepulse inhomogeneity.

The two-dimensional numerical code ATLANT [13] includes a Lagrangian description of one fluid two temperature hydrodynamics model,

$$\frac{d\rho}{dt} = -\rho \cdot \nabla \mathbf{v} \tag{1}$$

$$\rho \frac{d\mathbf{v}}{dt} = -\nabla (P_e + P_i) \tag{2}$$

$$\frac{dE_e}{dt} = -P_e \nabla \mathbf{v} + \nabla (\lambda_e \nabla T_e) - Q_{ei} - R_{rad} + \nabla \mathbf{S} \tag{3}$$

$$\frac{dE_i}{dt} = -P_i \nabla \mathbf{v} + \nabla (\lambda_i \nabla T_i) + Q_{ei}, \tag{4}$$

where ρ and $\mathbf{v}$ are the plasma density and velocity, E_e and E_i represent the electron and the ion internal energy density, P_e and P_i stand for the electron and the ion pressure, and T_e and T_i are the electron and the ion temperature, respectively. Both the classical and the flux limited electron heat conductivity λ_e is included in the electron energy conservation, while the ion heat conductivity λ_i is assumed to be classical. The electron-ion relaxation Q_{ei} is treated in the Spitzer approximation, and R_{rad} represents the energy loss by the bremsstrahlung emission; $\mathbf{S}$ is the energy flux density of laser radiation (Poynting vector). For simplicity we assume a constant mean ion charge $Z = 12$ for the aluminum, and an ideal gas equation of state.

Laser absorption is assumed to be collisional with the absorption rate k_{abs}, and the absorbed power density is governed by the following equation:

$$\left(\frac{\mathbf{S}}{|\mathbf{S}|}, \nabla \right) \mathbf{S} = k_{abs} \cdot \mathbf{S}, \tag{5}$$

The propagation of the laser beams inside a plasma is solved by means of a ray-tracing algorithm, described in detail in Ref. [15]. As the spatial resolution of the hydrocode is not sufficient for an exact calculation of laser absorption, we assumed a full absorption of the laser radiation entering the cell of the hydrocode, where the ray is reflected. In order to account for the estimated experimental absorption efficiency [16], the incident prepulse intensity is multiplied by the coefficient $\eta_2 = 0.5$, while the intensity of the main blue pulse is multiplied by $\eta_3 = 0.7$.

The bremsstrahlung x-ray emission in the direction parallel to the target surface is calculated in order to provide a comparison with the time-integrated pinhole camera pictures, recorded in the experiment [12]. The cutoff energy 0.6 keV of the x-ray filter, placed in front of the pinhole camera, is taken into account. An optically thin plasma for the continuum emission is assumed, as typically the Rosseland mean free path is ~ 0.7 cm for Al plasma with a density 2.7 g/cm^3 and temperature 0.6 keV. Thus the mean free path exceeds the transverse dimension of plasma by at least two orders of magnitude. The time integrated emissivity in the normal direction from any plane, including the axis of symmetry (in the spectral region limited by the cutoff of x-ray filter), is given by the integral

$$I(z,r) = 2.4 \times 10^{14} \int Z^3 \rho^2(z,r,t) \sqrt{T_e(z,r,t)} \times \exp\left(-\frac{0.6}{T_e(z,r,t)} \right) dt \ \ \text{J/cm}^3, \tag{6}$$

where an Al target is assumed, and z is the axial coordinate along the propagation of laser beams.

III. RESULTS

Our numerical simulations were inspired by the experimental results of Ref. [12]. Pinhole camera pictures, re-

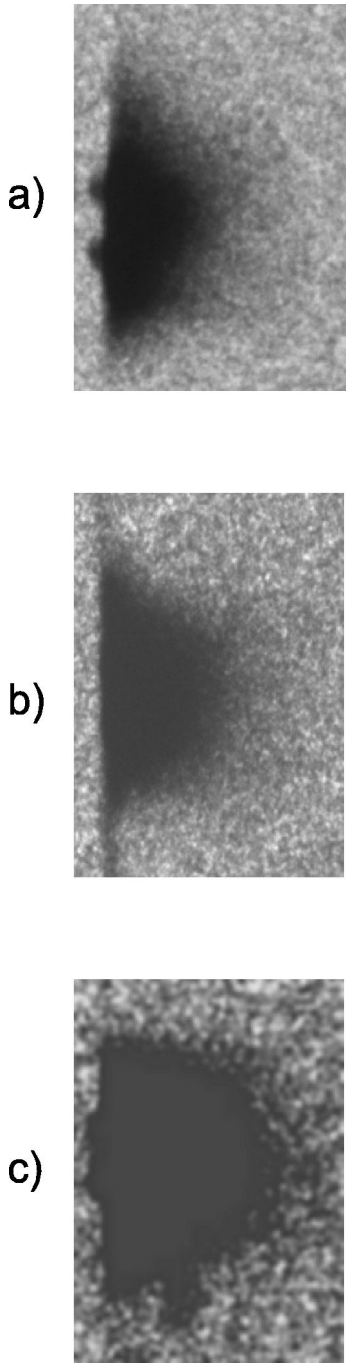

FIG. 2. Time integrated pinhole camera pictures of the plasma (side-on view) for delays of 0 (a), 0.5 ns (b), and 1 ns (c) between the prepulse and the main pulse. The laser is incident from the right, and the distance between the spot centers on the foil rear side in (a) is 80 μm, equal to the distance between the centers of the main pulse focal spots.

corded in a side-on view in experiments with respective delays of $\Delta t=0$, 0.5, and 1 ns between the maxima of the prepulse and of the main pulse, are presented in Fig. 2. The picture [Fig. 2(a)] taken without the delay $\Delta t=0$ ns clearly demonstrates an inhomogeneity in the x-ray emission on the rear side of the foil. The distance of the bumps on the side-on view exactly matches the distance of the centers of the two blue foci. When a prepulse advancing by 0.5 ns is used, smooth shapes of the x-ray emission are obtained [Fig. 2(b)], and the nonuniformity in the heating laser pulse cannot be detected by the pinhole cameras. The smoothing effect of the red beam depends essentially on the Δt delay between the prepulse and the main pulse. When $\Delta t=0$ (no delay), the situation is practically the same as with no laser prepulse. On the other hand, when the delay is too large, the smoothing effect is reduced and the nonuniformities in the x-ray emission may again be detected by the pinhole camera for $\Delta t=1$ ns [Fig. 2(c)]. The same dependence of the smoothing effect on the main pulse Δt delay can also be seen in the pinhole camera pictures taken from the rear-side view, presented in Ref. [12]. Two maxima, corresponding to the main pulse focal spots, are observed for the delays $\Delta t=0$ and 1 ns only.

Based on the parameters of the experiment [12], the peak intensity in the center of the incident main pulse is chosen as $I_b=5.9\times10^{14}$ W/cm^2, while the peak intensity of the prepulse is $I_r=4.4\times10^{13}$ W/cm^2. Both the laser prepulse and the main pulse are assumed Gaussian, 0.5 ns (full width at half maximum) long. The Gaussian radial profile $S_0\sim\exp(-r^2/r_0^2)$ of the incident main pulse is assumed to have $r_0=15.76$ μm; that means 80% of laser energy is contained inside a radius of 20 μm. We also conducted simulations with a Gaussian radial distribution of the prepulse with $r_0=60$ μm, and found only minor differences in the plasma dynamics in the central part ($r<60$ μm) of the target from the simulations with a uniform prepulse distribution and a simulation box with a radius $R=60$ μm. This confirms that the focal spot of the prepulse in the experiment [12] is large enough for the finite radius of the laser prepulse not to influence the thermal smoothing. Here we present mainly the results for the uniform radial distribution of the prepulse intensity, as they can be employed to demonstrate more readily the physics of the thermal smoothing of the ablation pressure. In addition, we give one example demonstrating that thermal smoothing is also effective with a nonuniform prepulse laser beam profile.

The position z_m of the target density maximum along the axial coordinate z is found for each value of (r,t). The surfaces $z_m(r)$ of the maximum compression are plotted in Fig. 3 for the specified times ($t=0$ is the temporal maximum of the main pulse). These surfaces represent a well defined position of the shock wave, and offer an easy possibility to follow its propagation. Practically no smoothing effect of the laser prepulse is observed [Fig. 3(a)], when the main pulse is incident simultaneously with the prepulse ($\Delta t=0$). When a suitable delay of the main pulse is chosen, the smoothing effect becomes apparent [Fig. 3(b), plotted for $\Delta t=0.5$ ns]. For a delayed main pulse, the shock wave induced by the main pulse needs some time to overtake the shock wave induced by the prepulse; thus no inhomogeneity is observed at the leading edge of the main pulse. However, for the delay $\Delta t=0.5$ ns, this occurs long before the main pulse maximum is reached. But even for this main pulse delay, some inhomogeneity in the shock wave propagation is later observed. However, its growth rate is cut down and the amplitude is reduced by an order of magnitude.

The influence of the main pulse delay on the shock-wave nonuniformity is even more clearly demonstrated in Fig. 4. Here the evolution of the difference $z_m(r=R)-z_m(r=0)$ between the shock wave position at the edge of the simula-

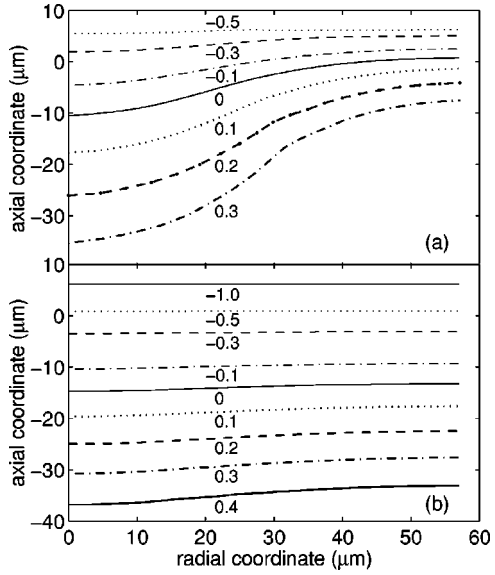

FIG. 3. Computed evolution of the maximum compression surface (shock-wave front) for the time delays $\Delta t=0$ ns (a) and $\Delta t=0.5$ ns (b) between the prepulse and the main pulse. Each curve represents a shock-wave front position at time t specified in nanoseconds by the curve label ($t=0$ coincides with the temporal maximum of the main pulse). The laser is incident along the axial coordinate from the upper side of the figures normally on the Al foil. The foil is initially placed between 7 and 0 μm on the axial coordinate parallel with the radial axis.

tion box and in the center of the focus (''shock-wave nonuniformity'') is presented for three values of the main pulse delay $\Delta t=0$, 0.5, and 1 ns. The smoothing effect is shown to be still significant for the maximum delay 1 ns, but it is less so for the medium 0.5-ns delay. The nonuniformity of the interaction starts to influence the shape of the maximum compression surface $z_m(r)$ only later, due to the late overtaking of the prepulse induced shock wave, but the nonuniformity after the main pulse maximum is larger than in the case of the medium delay. Thus, the existence of an optimum delay for smoothing by a laser prepulse is shown, and the value $\Delta t=0.5$ ns seems to be a reasonable estimate of the optimum delay in the conditions of the experiment [12].

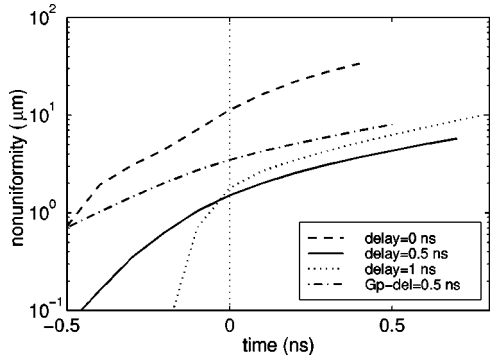

FIG. 4. Evolution of the longitudinal inhomogeneity size (bulging) for the prepulse with a uniform radial profile and three different time delays between the prepulse and the main pulse. The dash-dotted curve (labeled ''Gp'') displays the inhomogeneity growth for the prepulse with a Gaussian radial profile and a delay of 0.5 ns. The zero on the x axis is the time of the main pulse maximum.

We have conducted simulations with a nonuniform prepulse in order to estimate the impact of large scale inhomogeneities in the laser prepulse on the uniformity of the target acceleration. As a Gaussian intensity distribution in the prepulse is assumed with a radius of 60 μm, the laser intensity at the edge ($r=60$ μm) of the simulation box is 56% of the intensity of that at the center. The average prepulse intensity is set equal to the case of a uniform prepulse. Unlike the experiment, the positions of the prepulse and the main pulse maxima coincide here, and, thus, the detrimental effect of a nonuniform prepulse is presumably overestimated in the simulations. The evolution of the nonuniformity in the target acceleration for a Gaussian prepulse and the optimum delay $\Delta t=0.5$ ns are displayed in Fig. 4 (dot-dashed curve, labeled ''Gp''). The nonuniformity of the target acceleration is relatively large after the prepulse, but its subsequent growth is moderate. Its growth during the main laser pulse is even slower than in the case of a uniform prepulse. A comparison with the case of a uniform prepulse and $\Delta t=0$ ns shows that thermal smoothing due to a laser prepulse with a longer laser wavelength is still remarkably efficient, even for nonuniform prepulses. This result suggests that long scale inhomogeneities in the prepulse do not impose a serious risk for the uniform target acceleration.

Short scale nonuniformities of the target acceleration may grow faster due to the Rayleigh-Taylor instability. Their growth rate may be estimated [17] by the formula $\gamma=0.9\sqrt{k g}-3 k V_a$. The estimates of foil acceleration ($g\simeq 4\times 10^{15}$ cm/s^2) and ablation velocity ($V_a\simeq 10^5$ cm/s) are taken from our simulations. Then the wavelength 7 μm ($k=9000$) of the fastest growing mode and its growth rate $\gamma=2.7\times 10^9$ s^{-1} are derived from the above formula. Therefore, the fastest growing nonuniformities are increased only 3.9 times during the interval 0.5 ns between the prepulse and the main pulse. As the variations in the foil thickness are below 0.1 μm and the level of short scale inhomogeneities inside the prepulse beam is below 50%, the level of the prepulse imposed short scale inhomogeneities of the target acceleration is probably rather small.

An increase in the distance between the critical and ablation surface is usually believed [12,14] to explain the smoothing effect of the laser prepulse. However, it follows from the modeling that the main difference induced by the laser prepulse is a substantial modification of the main pulse absorption. Since a sufficiently long and dense plasma is formed by the prepulse, the main pulse radiation is absorbed not only in the vicinity of the critical surface, but a substantial part of the laser energy is also absorbed in the underdense plasma. This fact is demonstrated in Fig. 5, where the profile of absorbed laser power along the central laser ray ($r=0$) is plotted at the main pulse maximum ($t=0$) for the three values of the main pulse delay. For an optimum delay, a long underdense plasma is present, inside which a significant laser absorption occurs. Thus a relatively dense, long, and hot layer of underdense plasma is formed where a large electron thermal conductivity induces a substantial thermal smoothing. In this situation, thermal smoothing might occur together with a reduced reflectivity of the main pulse by collisional absorption, and this could be verified experimentally or observed in the simulations where a detailed model of laser reflection is introduced. In reality, the favorable situ-

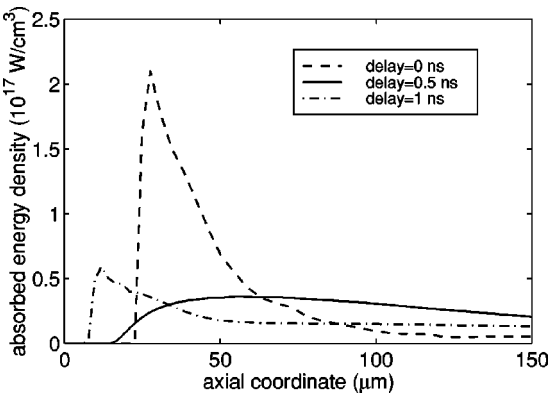

FIG. 5. Absorbed laser power at the symmetry axis $r=0$ in the moment of the main pulse maximum ($t=0$) vs the axial coordinate for three different delays (the initial position of the Al foil is between 0 and 7 μm).

ation of enhanced collisional absorption might, however, be offset by light scattering from the long scale plasma formed by the prepulse due to nonlinear processes such as Raman scattering. It should also be noted that the thermal flux limitation does not influence our results when the flux limiter $f \gtrsim 0.05$ is used.

The bremsstrahlung x-ray emission is calculated in order to find out the conditions when nonuniformities in the laser target interaction are observable in time integrated pictures taken by a pinhole camera from a side-on view. Here the geometrical factor, due to the cylindrical symmetry, is not taken into account, as the cylindrical symmetry of the simulation does not correspond exactly to the geometry of the side-on view of the pinhole camera in the experiment (Fig. 2). Thus, in the assumed approximation, the time integrated intensity in the x-ray image is proportional to the integrated x-ray emissivity I, given by Eq. (6). The value of this integral, calculated in our numerical simulations, is plotted in Fig. 6 for all the three values of the main pulse delay Δt. For the medium delay $\Delta t=0.5$ ns [Fig. 6(b)], no nonuniformities (inhomogeneities in transverse direction) may be observed in the x-ray image. Although thermal smoothing does not completely remove all the nonuniformities in the foil acceleration even for this Δt [see Figs. 3(a) and 4], these nonuniformities emerge somewhat later, when the plasma is too cold to emit in the spectral region above the cutoff of the x-ray filter. For the maximum delay $\Delta t=1$ ns, the nonuniformities in the x-ray image (Fig. 6c) are reduced substantially, compared with no delay $\Delta t=0$ [Fig. 6(a)], but they are still apparent in our numerical results. The nonuniformities develop in this particular case further inside the plasma, because the perturbations have more time to develop under the combined action of the prepulse followed by a more distant main pulse. These results are in a reasonable agreement with an experiment in which the nonuniformities are observed for delays of 0 and 1 ns, but no nonuniformity is detected for the delay $\Delta t=0.5$ ns. However, the calculated nonuniformities for the maximum main pulse delay seem to be slightly underestimated, as compared with the experiment.

IV. CONCLUSIONS

Smoothing of the ablation pressure by the laser prepulse has been studied by 2D hydrodynamics simulations. It is

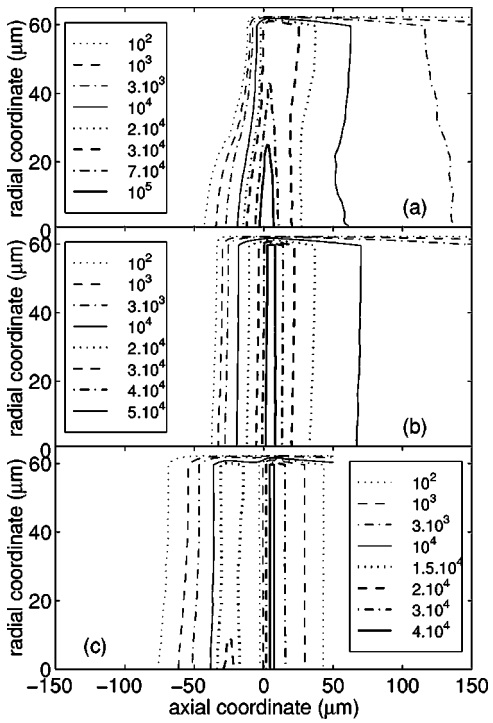

FIG. 6. Computed integrated x-ray images. Contours of integrated x-ray emissivity in J/cm^3 are plotted for the time delays $\Delta t=0$ ns (a), 0/5 ns (b), 1 ns (c). The laser is incident from the right, and the initial position of the Al foil is from 0 to 7 μm. Thanks to the larger distance of the prepulse from the main pulse, the overall time of the target motion is longest for a delay of 1 ns, and, thus, the target shift is the largest one.

shown that under the given conditions illumination inhomogeneities with transverse dimensions at least up to 30 μm may be smoothed out. The existence of an optimum delay Δt between the prepulse and the main laser pulse has been demonstrated. The smoothing effect is very significant for a suitable Δt delay; the growth of inhomogeneities in the ablation pressure is delayed and reduced by an order of magnitude. Even for such a delay of the main pulse, the inhomogeneities in the ablation pressure are not fully suppressed. However, no nonuniformities may be observed in the plasma by a standard time integrated x-ray diagnostics, as they emerge only after the main laser pulse when the plasma is too cold to emit energetic x rays.

Our simulations reveal that the laser radiation of the main pulse is absorbed efficiently in an underdense plasma far from the critical surface, since a relatively long density profile is formed by the prepulse for the optimum delay of the main pulse. Thus the distance between the laser absorption region and the ablation surface is enlarged, and a large scale length layer of relatively hot and dense plasma is formed where the role of electron thermal conductivity is enhanced to induce an important thermal smoothing. Consequently, such a laser prepulse should enhance absorption of the main laser pulse; however, on the other hand, it should reduce hydroefficiency.

A good qualitative agreement is found between the results of numerical simulations and the experiment [12]. Both the experiment and simulations show the best smoothing when the main pulse is delayed by 0.5 ns. The smoothing effect is

very significant for this delay, and can lead to an important reduction in the nonuniformity of the acceleration of shell targets. Thus we show that thermal smoothing by a suitable laser prepulse may be a useful method, meeting the requirements on ablation pressure uniformity necessary for inertial fusion.

ACKNOWLEDGMENTS

The work of J.L. and the visit of A.I. to Prague was supported by Grant No. 202/97/1186 from the Grant Agency of the Czech Republic. K.M. and K.R. were supported by Grant No. 202/96/1688 from the same agency.

[1] B. Meyer, J. Appl. Phys. **53**, 2947 (1982).
[2] M. Desselberger, M. W. Jones, J. Edwards, M. Dunne, and O. Willy, Phys. Rev. Lett. **74**, 2961 (1995).
[3] E. G. Gamaly, A. P. Favorsky, A. O. Fedyanin, I. G. Lebo, E. E. Myshetskaya, V. B. Rozanov, and V. F. Tiskin, Laser Part. Beams **9**, 399 (1980).
[4] T. R. Boehly, V. A. Smalyuk, D. D. Meyerhofer, J. P. Knauer, D. K. Bradley, R. S. Craxton, M. J. Guardalben, S. Skupsky, and T. J. Kessler, J. Appl. Phys. **85**, 3444 (1999).
[5] J. H. Gardener and S. E. Bodner, Phys. Rev. Lett. **47**, 1137 (1981).
[6] M. Dunne, M. Borghesi, A. Iwase, M. W. Jones, R. Taylor, O. Willy, R. Gibson, S. R. Goldman, J. Mack, and R. G. Watt, Phys. Rev. Lett. **75**, 3858 (1995).
[7] R. G. Watt, J. Duke, C. J. Fontes, P. L. Gobby, R. V. Hollis, R. A. Kopp, R. J. Mason, D. C. Wilson, C. P. Verdon, T. R. Boehly, J. P. Knauer, D. D. Meyerhofer, V. Smalyuk, and R. P. J. Town, Phys. Rev. Lett. **81**, 4644 (1998).
[8] J. D. Sethian, S. E. Bodner, D. G. Colombant, J. P. Dahlburg, S. P. Obenschain, C. J. Pawley, V. Serlin, J. H. Gardner, Y. Aglitskiy, Y. Chan, A. V. Deniz, T. Lehecka, and M. Klapisch, Phys. Plasmas **6**, 2089 (1999).
[9] T. Boehly, M. Russotto, R. S. Craxton, R. Epstein, B. Yaakobi, L. B. Da Silva, J. Nilsen, E. A. Chandler, D. J. Fields, B. J. McGowan, D. L. Matthews, J. H. Scofield, and G. Shimkaveg, Phys. Rev. A **42**, 6962 (1990).
[10] J. Nilsen, B. J. McGowan, L. B. Da Silva, and J. C. Moreno, Phys. Rev. A **48**, 4682 (1993).
[11] J. Moreno, J. Nilsen, and L. B. Da Silva, Opt. Commun. **110**, 585 (1994).
[12] K. Mašek, B. Králiková, L. Láska, S. Přeučil, K. Rohlena, J. Skála, P. Straka, A. V. Bessarab, S. G. Garanin, Yu. F. Kiryanov, G. G. Kochemasov, L. V. Lvov, A. B. Ryadov, S. A. Sukharev, N. A. Suslov, O. A. Vinokurov, and A. I. Zaretskiy, Proc. SPIE **2767**, 91 (1996).
[13] I. G. Lebo, I. V. Popov, V. B. Rozanov, and V. F. Tishkin, J. Russ. Laser Res. **15**, 136 (1994).
[14] I. G. Lebo, K. Rohlena, V. B. Rozanov, and V. F. Tishkin, Kvant. Elektron. **23**, 71 (1996) [Quantum Electron. **26**, 69 (1996)].
[15] A. B. Iskakov, I. G. Lebo, I. V. Popov, V. B. Rozanov, and V. F. Tishkin, Kratk. Soobsch. Fiz. No. 1-2, 28 (1997) [Bull. Lebedev Phys. Inst. No. 1, 23 (1997)].
[16] K. Eidmann, F. Amiranoff, R. Fedosejevs, A. G. M. Maaswinkel, R. Petsch, R. Sigel, G. Spindler, Yung-lu Teng, G. Tsarikis, and S. Witkowski, Phys. Rev. A **30**, 2568 (1984).
[17] H. Takabe, K. Mima, L. Montierth, and R. L. Morse, Phys. Fluids **28**, 3676 (1985).